

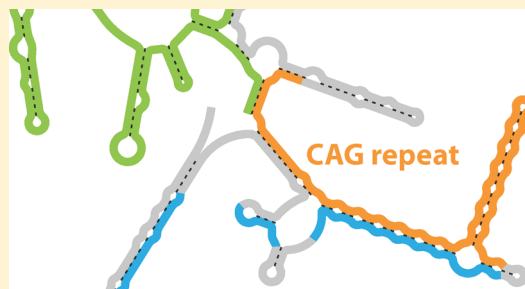
Role of Context in RNA Structure: Flanking Sequences Reconfigure CAG Motif Folding in *Huntingtin* Exon 1 Transcripts

Steven Busan and Kevin M. Weeks*

Department of Chemistry, University of North Carolina, Chapel Hill, North Carolina 27599-3290, United States

S Supporting Information

ABSTRACT: The length of the CAG-repeat region in the *huntingtin* mRNA is predictive of Huntington's disease. Structural studies of CAG-repeat-containing RNAs suggest that these sequences form simple hairpin structures; however, in the context of the full-length *huntingtin* mRNA, CAG repeats may form complex structures that could be targeted for therapeutic intervention. We examined the structures of transcripts spanning the first exon of the *huntingtin* mRNA with both healthy and disease-prone repeat lengths. In transcripts with 17–70 repeats, the CAG sequences base paired extensively with nucleotides in the 5' UTR and with conserved downstream sequences including a CCG-repeat region. In *huntingtin* transcripts with healthy numbers of repeats, the previously observed CAG hairpin was either absent or short. In contrast, in transcripts with disease-associated numbers of repeats, a CAG hairpin was present and extended from a three-helix junction. Our findings demonstrate the profound importance of sequence context in RNA folding and identify specific structural differences between healthy and disease-inducing *huntingtin* alleles that may be targets for therapeutic intervention.



Huntington's disease (HD) is a devastating, ultimately fatal neurodegenerative disorder. In healthy individuals, the first exon of each of the two alleles of the *huntingtin* gene contains a relatively short region of CAG triplet repeats that encode polyglutamine; the most common allele has 17 repeats. In HD patients, one *huntingtin* allele is abnormally expanded to contain between 36 and 70 CAG repeats, although patient alleles with shorter or significantly longer repeat regions have also been reported.^{1,2} The length of this HD-expanded CAG-repeat region is inversely correlated with patient age at the onset of symptoms, which include involuntary movements and dementia.² Pathogenesis is due to the polyglutamine peptides translated from the disease allele, and the expanded CAG repeat-containing RNA transcripts may also be toxic.^{3,4}

This study was motivated by the potential for allele-selective therapeutic targeting of the *huntingtin* mRNA that might result if the RNA structure could be modeled with confidence. Huntingtin is nearly universally expressed and appears to be especially important for correct functioning of the adult nervous system.^{5–8} An ideal therapeutic would therefore specifically destroy the disease-expanded *huntingtin* transcript or block its translation while preserving the function of the healthy length transcript. Recent efforts to selectively target the expanded *huntingtin* transcript have focused either on targeting single-nucleotide polymorphisms associated with disease alleles^{9,10} or on targeting the CAG repeats, taking advantage of the greater number of effective binding sites in the expanded transcript.¹¹ Allele-specific structures within the *huntingtin* mRNA could provide additional, and more precise, targets for therapeutic development.

Biochemical studies have consistently demonstrated that RNA transcripts containing CAG repeats fold into duplex helices and hairpins.^{12–15} CAG-containing duplexes have been examined by NMR¹⁴ and X-ray crystallography.¹⁶ Recent studies have also shown that flanking sequences can modulate triplet-repeat folding. The addition of even a short region of flanking *huntingtin* sequence to CAG repeats results in the formation of more complex structures.¹⁷ We therefore sought to determine the folded structures of *huntingtin* transcripts with varying CAG repeat lengths in the context of the sequence of longer transcripts, more closely resembling those found in cells.

We designed five transcripts covering the entire first exon of the *huntingtin* mRNA. These exon 1 transcripts spanned the 5' untranslated region (UTR), contained from 17 to 70 CAG repeats, and included the downstream region encoding polyproline repeats (mostly CCG). A combination of SHAPE (selective 2'-hydroxyl acylation analyzed by primer extension), RNase T1 cleavage, and targeted antisense oligonucleotide binding was used to investigate the folded structures of these transcripts. We found that the sequence context had profound effects on the folded structure of the transcript because CAG repeats pair extensively with flanking *huntingtin* mRNA sequences. A CAG hairpin was absent or short in *huntingtin* transcripts with repeat lengths typical of healthy individuals (17 and 23 repeats) but was present in transcripts with disease-associated numbers of repeats (36, 41, and 70 repeats). Our

Received: August 17, 2013

Revised: October 17, 2013

Published: November 7, 2013



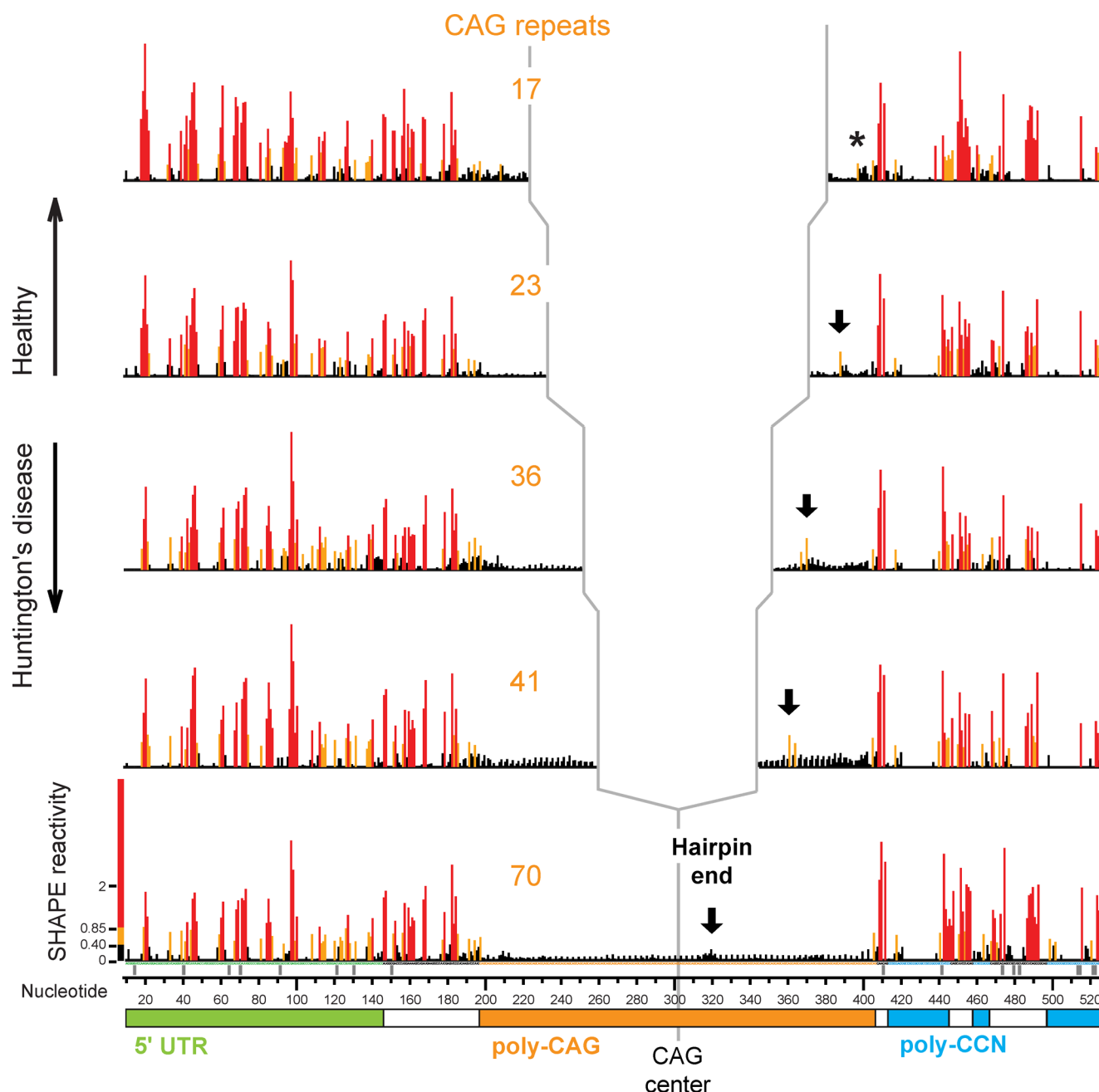


Figure 1. SHAPE profiles for *huntingtin* exon 1 transcripts as a function of CAG-repeat length. Reactivity profiles are shown split in the center of the CAG repeat region and aligned at the 5' and 3' ends. The black, yellow, and red scale indicates low, medium, and high SHAPE reactivities, respectively. The most SHAPE-reactive region within the CAG repeat consistently falls six CAG repeats 3' of the CAG-repeat-region center, as emphasized with solid arrows. The region likely to form an internal loop in the 17-CAG repeat transcript is indicated with an asterisk (top panel). Data shown are the average of three independent experiments. The small number of nucleotides for which no data were obtained (because of strong electropherogram peaks in the no-reagent control, see Methods) are marked with gray boxes on the x axis.

data suggest that there are structural differences between healthy and disease-inducing alleles that may be promising targets for therapeutic intervention.

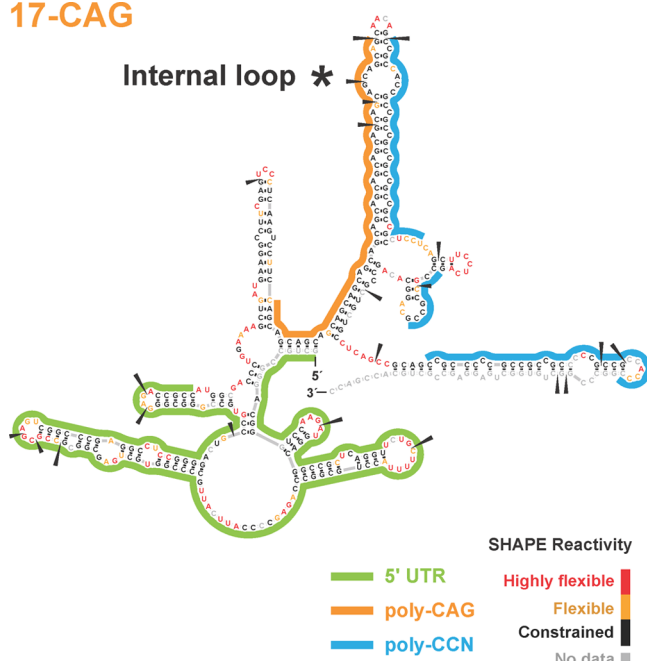
METHODS

Sequences, Primers, and Antisense Oligonucleotides.

The sequence of the *huntingtin* mRNA exon 1 transcript is as follows ($n = 17, 23, 36, 41$, and 70): GCUGCCGGGA CGGGUCCAAG AUGGACGGCC GCUCAGGUUC UGCUUUUACC UGCGGCCAG AGCCCCAUUC AUUGCCCCGG UGCUGAGCGG CGCCGCGAGU

CGGCCCGAGG CCUCCGGGGA CUGCCGUGCC GGGCGGGAGA CCGCAUUGG GACCCUGGAA AAGCUGAUGA AGGCCUUCGA GUCCCUCAAG UC-CUUC (CAG) $_n$ CAACAGCCGC CACCGCCGCC GCCGC-CGCCG CCGCCUCCUC AGCUUCCUCA GCCGC-CGCCG CAGGCACAGC CGCUGCUGCC UCAGC-CGCAG CCGCCCCCGC CGCCGCCCCC GCCGCCACCC GGCCCGGCUG UGGCUGAGGA GCCGUGCAC CGACC. The reverse-transcription primer is GGTCGGTGCAGCG, and the antisense oligonucleotides, listed by the 5'-most target nucleotide in the 70-CAG

17-CAG



41-CAG

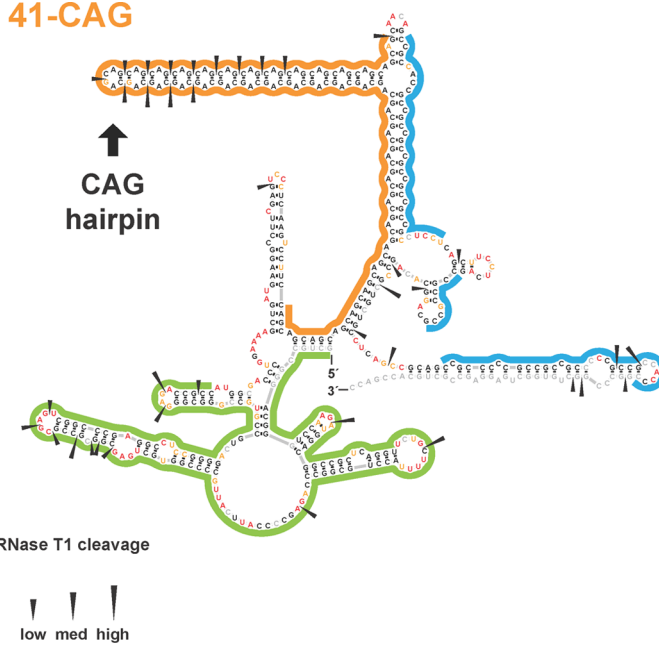


Figure 2. Structural models for representative normal and disease-associated *huntingtin* transcripts. Secondary-structure models for the most common healthy length transcript (17-CAG) and for a strongly disease-associated (41-CAG) RNA are shown. SHAPE and T1 RNase probing are shown with colored nucleotides and arrowheads, respectively. The absence of a CAG hairpin in the 17-CAG repeat RNA is emphasized with an asterisk.

huntingtin transcript (* indicates a “locked” nucleotide¹⁸) are (1) *TCC*CGG*CAG*C, (159) *ATC*AGC*TTT*T, (431) *AGG*AGG*CG*GCG*GCG*G, (464) *GTG*CCT*GCG*G, and (475) *TGA*GGC*AG*-CAG*CGG*C.

Transcript Production and Purification. Plasmids contained *huntingtin* sequences, a T7 promoter at the 5′ end, and a Bts I restriction site at the 3′ end and were obtained by de novo synthesis (Blue Heron Biotechnology). Cells (SURE 2, Agilent Technologies) were transfected with plasmid, and 500 mL cultures were prepared. Plasmids were extracted, and constructs were verified by sequencing. Plasmids were linearized with Bts I (New England Biolabs), and linearization was confirmed by agarose gel electrophoresis. Linearized template sequences were transcribed using T7 RNA polymerase, and products were separated by polyacrylamide gel electrophoresis, excised from the gel, and recovered by precipitation with ethanol.¹⁹ Transcripts were resuspended at 0.25 μM in 1/2× TE buffer, aliquoted for single use, and stored at −20 °C.

In Vitro Transcript Folding, SHAPE, and RNase T1 Probing. Transcripts were denatured at 95 °C for 2 min, snap-cooled on ice for 2 min, and refolded at 37 °C for 30 min in 50 mM Tris-HCl (pH 8), 75 mM KCl, and 3 mM MgCl₂. SHAPE probing was performed using 5–8 mM final concentration 1-methyl-7-nitroisatoic anhydride (1M7) for 5 min at 37 °C.²⁰ Enzymatic cleavage was carried out using RNase T1 (Ambion) at a final concentration of 0.2 U/μL for 5 min at 37 °C. Transcripts were recovered by ethanol precipitation. SuperScript III reverse transcriptase (Invitrogen) was used to extend the fluorescently labeled reverse-transcription primer (above) for 1 h at 37 °C. Fluorescent cDNA fragments were quantified using capillary electrophoresis.²¹

Structure Disruption Using Antisense Oligonucleotides. Transcripts were combined with five pooled antisense

oligonucleotides (ASOs), containing locked nucleotides (Exiqon) to enhance RNA binding, at a 4-fold excess of each ASO over RNA. Transcripts were then denatured, snap-cooled, folded, and modified as described above. To reduce the concentration of ASOs prior to reverse transcription, transcripts were incubated with three DNA oligonucleotides complementary to ASOs 431, 464, and 475 at a high concentration (200 times that of the RNA) at 95 °C for 2 min. Three serial rounds of binding, washing, and elution (RNeasy MinElute columns, Qiagen) were then performed to remove the ASOs and their complements. Structure analysis by reverse transcription was performed as outlined above.

Electropherogram Analysis and Structure Prediction. Electropherograms were analyzed with QuShape.²¹ SHAPE data were analyzed as follows: nucleotides with no-reagent signals above the 99th percentile in any trial were excluded from analysis in all transcript data sets. SHAPE reactivity profiles were normalized as described,²² except that the CAG-repeat region was excluded from the normalization calculation to maintain a consistent SHAPE reactivity distribution across all transcripts. RNase T1 data were analyzed as follows: nucleotides with background signals in the top 3% were excluded. Background and plus-RNase signals were normalized to the median of the plus-RNase signal. After background subtraction, guanosine residues showing normalized intensity values between 1 and 2 were designated low cleavage, between 2 and 4, medium cleavage, and above 4, high cleavage.

Secondary structures were modeled using the Fold module of RNAstructure,²³ version 5.4, using the latest parameters for incorporating SHAPE data.^{24,25} Because the *huntingtin* mRNA likely forms many noncanonical base pairs and contains multiple regions of repeated sequence, structure modeling was challenging. Without constraining secondary-structure models with SHAPE data, RNAstructure predicted a large number of alternative structures of similar energy. SHAPE

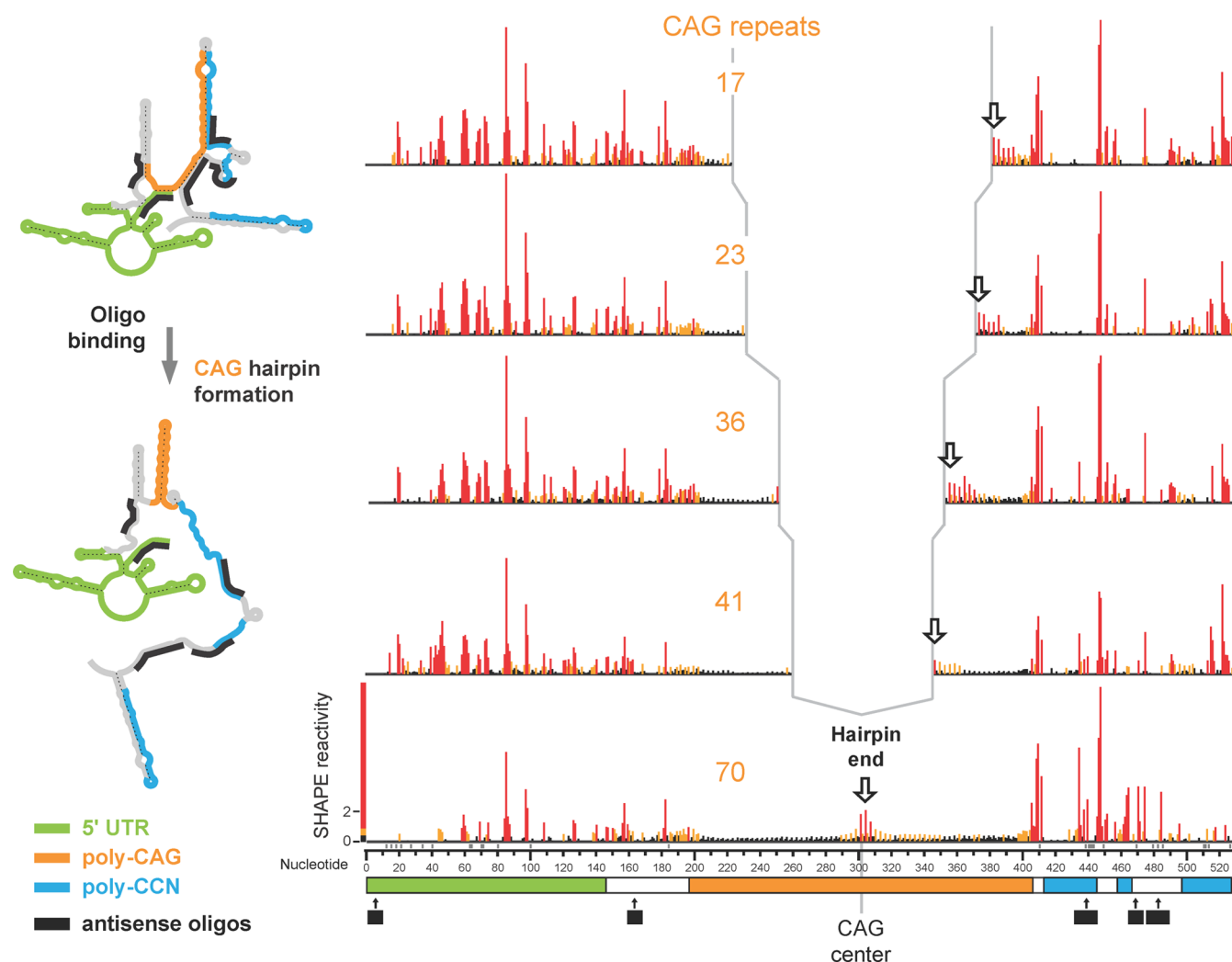


Figure 3. SHAPE analysis of *huntingtin* transcripts in the presence of antisense oligonucleotides designed to disrupt pairing between CAG sequences and flanking regions. Five antisense oligonucleotides were designed to bind specific, non-CAG sequences in the *huntingtin* mRNA to disrupt base pairing with the CAG-repeat region and to promote formation of a CAG hairpin. Oligonucleotide binding sites are shown with black bars. The center (reactive) region of each CAG-repeat element is emphasized with an open arrow and is consistent with simple hairpin formation by self-paired CAG sequences.

constraints brought these predictions into agreement with experimental data and significantly reduced the number of plausible structures. Given the overall similarities in nucleotide reactivities across the five transcripts (Figures 1 and 3 and Supporting Information Figure 1), the lowest predicted free-energy structure for the shortest transcript was used as a template to select the most likely structure for each of the CAG-expanded transcripts. In addition, we selected those structural models that showed reactive nucleotides in the CAG-repeat region within two triplets of a CAG hairpin terminus.

RESULTS

SHAPE and RNase Probing of *Huntingtin* Exon 1. We used SHAPE^{26,27} chemical probing to analyze the structure of five RNA transcripts containing shorter CAG-repeat lengths (17 and 23 repeats) typical of healthy alleles and longer, disease-associated, numbers of repeats (36, 41, and 70 repeats). Little degradation of RNAs was observed as judged by the low peak intensities in reverse-transcription products from the no-reagent controls, as analyzed by capillary electrophoresis. SHAPE reactivity profiles for each of the transcripts are

shown split in the center of the CAG-repeat region and aligned at the 5' and 3' ends (Figure 1). Overall, SHAPE reactivity profiles for the five transcripts are highly similar, suggesting that the global secondary structure is not affected by expanded CAG repeats (Figure 1). Within the CAG-repeat region in each transcript, most nucleotides were unreactive, consistent with formation of stable base pairing.^{26,27} In addition, within each CAG repeat region, there was a short region with more reactive (conformationally flexible) nucleotides; this region was not centered in the CAG-repeat region but instead was offset in the 3' direction (Figure 1, emphasized with solid arrows). This asymmetry in the CAG-repeat regions was also observed by RNase T1 enzyme probing (Supporting Information Figure 1). The group of SHAPE-reactive nucleotides was consistently located six triplets 3' of the center of the poly-CAG repeat.

Structural Models of *Huntingtin* Transcripts. We used the SHAPE data to develop experimentally supported^{24,25} models for thermodynamically accessible states for each of our *huntingtin* RNA transcripts. The 5' UTR and 3' regions of the RNAs are predicted to form similar or identical structures, independent of CAG-repeat length (Figure 2). In general, these

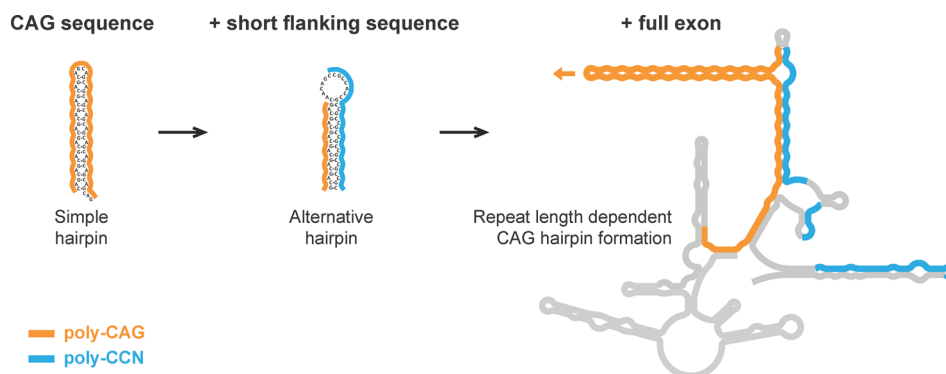


Figure 4. Role of flanking sequence in defining CAG-repeat RNA structures. Shown are secondary-structure models for the CAG-repeat sequence,¹² for a CAG repeat with short flanking sequences,¹⁷ and for the full-length *huntingtin* exon 1 sequence studied in this work. A CAG hairpin begins to form with intermediate-length repeat expansion and preferentially forms a long classical hairpin (shown) with disease-associated CAG expansions.

structural models are well-defined (Supporting Information Figure 2). These models, which are based on RNA transcripts with long flanking sequences, likely capture features relevant to *huntingtin* mRNA structure in vivo. The 5' end corresponds to the transcription start site –145 nucleotides from the translation start, although transcripts starting at –135 may also be present in vivo.^{28,29} Some end effects are possible because of truncation of the studied transcripts at the 3' exon boundary (155 nucleotides from the CAG-repeat region).

Strikingly, the CAG repeat region forms extensive base-pairing interactions with nucleotides outside the repeat region (Figure 2 and Supporting Information Figure 2, CAG repeat sequences are highlighted in orange). The 5' end of the UTR, the CCG-repeat region immediately downstream of the CAG-repeat region, and an 11-nucleotide region with the sequence GCCGCUGCUGC (perfectly complementary to CAG repeats apart from one A:C mismatch) are all predicted to base pair with CAG-repeat nucleotides. The remarkable result of this base pairing is that a hairpin formed only of CAG-repeat nucleotides is entirely absent from the model of the healthy *huntingtin* transcript that contains 17 CAG repeats (Figure 2, left). Moreover, the CAG-repeat hairpin and the three-helix junction from which it extends represent allele-specific structures that occur preferentially in the longer disease-associated alleles.

CAG Hairpin Induction. If base pairing between CAG repeats and flanking sequences prevents CAG hairpin formation in healthy-length *huntingtin* transcripts, disrupting this base pairing should allow the RNA to refold and form extended hairpins (Figure 3, left). We folded all five *huntingtin* transcript RNAs in the presence of five antisense oligonucleotides designed to bind sequences flanking the CAG repeats and to compete for base pairing with these non-CAG sequences. Under these conditions, SHAPE-reactive nucleotides occurred at or near the center of the CAG-repeat element in all transcripts, both healthy length and disease expanded (Figure 3, right, site of hairpin loop is emphasized with open arrow). Thus, CAG-repeat elements can be forced to form a simple hairpin structure by inhibiting pairing to flanking sequences present in the native transcript.

DISCUSSION

Our work provides the first empirical examination of *huntingtin* mRNA structure in the context of extended, native flanking sequences (in this case, the entire first exon). Given the GC-rich nature of the *huntingtin* mRNA, it is not surprising that the

transcripts are highly structured (Figure 2). The CAG-repeat regions adopt distinct structures that depended on repeat length and on the flanking sequence context (Figure 4). In the absence of interacting flanking sequences, poly-CAG transcripts, which are found in several disease-related contexts,^{30,31} fold back on themselves to base pair into simple hairpins.^{12,13} In *huntingtin* exon 1 mRNA sequences, CAG repeats are followed by poly-CCN sequences and a complementary GCCGCUGCUGC sequence, and our analysis indicates that these flanking sequences pair with the poly-CAG element. Because CAG repeats base pair with flanking sequences, a CAG hairpin was not observed in the transcript containing the 17 CAG repeats typical of a healthy individual.

Cellular and animal models of HD indicate that disease symptoms correlate with several factors including repeat lengths, expression levels, localization of *huntingtin* transcripts, truncation of the *huntingtin* sequence, and stoichiometry of native and mutant sequences.^{32–34} This work supports the hypothesis that the CAG-repeat-containing transcript itself, and not just its ability to encode polyglutamine, might be important for disease etiology. The two widely used mouse models of HD employ a yeast artificial chromosome (YAC128)³⁵ or a bacterial artificial chromosome (BACHD).³⁶ Despite expressing similar mutant *huntingtin* mRNAs, BACHD mice do not show aggregate formation or display the transcriptional dysregulation present in YAC128 mice and HD patients.³⁷ An important distinction between these models is the use of nearly pure CAG repeats in YAC128 versus unnatural, mixed CAA/CAG repeats in BACHD. The presence of CAA triplets disrupts extended hairpin formation and favors branched secondary structures.³⁸ In addition, CAA sequences will not base pair strongly with CCG sequences and other flanking regions present in the authentic *huntingtin* transcript sequence. The allele used in the BACHD model will almost certainly lack the striking CAG-repeat-length-dependent hairpin formation found in this study; therefore, some of the phenotypic differences that distinguish pure CAG from mixed-codon HD models may reflect differences in RNA structure.

The secondary-structure models developed in this work also suggest specific roles for *huntingtin* mRNA structure in splicing and translation. First, expanded CAG repeats within *huntingtin* transcripts contribute to misregulation of splicing. These defects include sequestration of the splicing factor muscleblind-like protein 1^{17,39} and mis-splicing of the *huntingtin* transcript, possibly because of recruitment of the splicing factor SRSF6.⁴⁰ We hypothesize that base pairing by healthy-length

CAG repeats to flanking sequences reduces deleterious recognition by splicing factors. Second, the *huntingtin* 5' UTR and the region surrounding the primary translation start site form stable RNA structures (Figure 2); in general, structured UTRs reduce translation initiation.⁴¹ Taken together with a putative active upstream open reading frame in *huntingtin*,²⁹ this work suggests that regulation of *huntingtin* translation may be complex and involve the interplay of the general translation-initiation machinery, contributions of strong local structure at the translation-initiation site, and the possible presence of multiple initiation sites.

The absence of a CAG hairpin in short, healthy-length *huntingtin* transcripts and its presence in transcripts with increased numbers of repeats suggests that allele-specific targeting of *huntingtin* mRNA structures will be possible. SHAPE-directed structure models suggest that CAG hairpins occur in disease-associated alleles but not in alleles with fewer repeats characteristic of healthy individuals. Molecules that bind specifically to CAG hairpins, especially if they discriminate against duplexes in which CAG sequences pair with CCG repeat sequences (Figure 2), are likely to be very selective for disease-causing alleles. The three-helix junction from which the CAG hairpin extends represents another novel RNA target with the potential for both gene and allele selectivity. Broadly, our findings highlight the importance of flanking sequence in RNA folding and hint at the insights to be gained by conducting quantitative, large-scale RNA-structure analyses. Examinations of the effects of context on RNA structure are likely to identify new therapeutic targets in repeat-expansion diseases.

■ ASSOCIATED CONTENT

■ Supporting Information

RNA structure probing profiles using RNase T1; secondary structure models for 23, 36, and 70-CAG repeat length *huntingtin* exon 1 transcripts; and plausible competing structures for long CAG repeat sequences. This material is available free of charge via the Internet at <http://pubs.acs.org>.

■ AUTHOR INFORMATION

Corresponding Author

*E-mail: weeks@unc.edu; Tel.: 919-962-7486.

Notes

The authors declare no competing financial interest.

■ ACKNOWLEDGMENTS

We are indebted to the CHDI Foundation for support of this work (E-0409 to K.M.W.).

■ REFERENCES

- (1) Kremer, B.; Goldberg, P.; Andrew, S. E.; Theilmann, J.; Telenius, H.; Zeisler, J.; Squitieri, F.; Lin, B.; Bassett, A.; Almqvist, E., et al. (1994) A worldwide study of the Huntington's disease mutation. The sensitivity and specificity of measuring CAG repeats. *N. Engl. J. Med.* 330, 1401–1406.
- (2) Lee, J. M.; Ramos, E. M.; Lee, J. H.; Gillis, T.; Mysore, J. S.; Hayden, M. R.; Warby, S. C.; Morrison, P.; Nance, M.; and Ross, C. A. (2012) CAG repeat expansion in Huntington disease determines age at onset in a fully dominant fashion. *Neurology* 78, 690–695.
- (3) Hsu, R. J.; Hsiao, K.-M.; Lin, M.-J.; Li, C.-Y.; Wang, L.-C.; Chen, L.-K.; and Pan, H. (2011) Long tract of untranslated CAG repeats is deleterious in transgenic mice. *PLoS One* 6, e16417-1–e16417-11.
- (4) Shieh, S. Y., and Bonini, N. M. (2011) Genes and pathways affected by CAG-repeat RNA-based toxicity in *Drosophila*. *Hum. Mol. Genet.* 20, 4810–4821.

(5) Velier, J., Kim, M., Schwarz, C., Kim, T. W., Sapp, E., Chase, K., Aronin, N., and DiFiglia, M. (1998) Wild-type and mutant huntingtin's function in vesicle trafficking in the secretory and endocytotic pathways. *Exp. Neurol.* 152, 34–40.

(6) Gauthier, L. R., Charrin, B. C., Borrell-Pagès, M., Dompierre, J. P., Rangone, H., Cordelières, F. P., De Mey, J., MacDonald, M. E., Lessmann, V., Humbert, S., et al. (2004) Huntingtin controls neurotrophic support and survival of neurons by enhancing BDNF vesicular transport along microtubules. *Cell* 118, 127–138.

(7) Caviston, J. P., and Holzbaur, E. L. F. (2009) Huntingtin as an essential integrator of intracellular vesicular trafficking. *Trends Cell Biol.* 19, 147–155.

(8) Zala, D., Hinckelmann, M. V., and Saudou, F. (2013) Huntingtin's function in axonal transport is conserved in *drosophila melanogaster*. *PLoS One* 8, e60162-1–e60162-10.

(9) Pfister, E. L., Kennington, L., Straubhaar, J., Wagh, S., Liu, W., DiFiglia, M., Landwehrmeyer, B., Vonsattel, J.-P., Zamore, P. D., and Aronin, N. (2009) Five siRNAs targeting three SNPs may provide therapy for three-quarters of huntington's disease patients. *Curr. Biol.* 19, 774–778.

(10) Carroll, J. B., Warby, S. C., Southwell, A. L., Doty, C. N., Greenlee, S., Skotte, N., Hung, G., Bennett, C. F., Freier, S. M., and Hayden, M. R. (2011) Potent and selective antisense oligonucleotides targeting single-nucleotide polymorphisms in the Huntington disease gene/allele-specific silencing of mutant huntingtin. *Mol. Ther.* 19, 2178–2185.

(11) Gagnon, K. T., Pendergraff, H. M., Deleavey, G. F., Swayze, E. E., Potier, P., Randolph, J., Roesch, E. B., Chattopadhyaya, J., Damha, M. J., Bennett, C. F., et al. (2010) Allele-selective inhibition of mutant huntingtin expression with antisense oligonucleotides targeting the expanded CAG repeat. *Biochemistry* 49, 10166–10178.

(12) Sobczak, K., de Mezer, M., Michiewski, G., Kroi, J., and Krzyzosiak, W. J. (2003) RNA structure of trinucleotide repeats associated with human neurological diseases. *Nucleic Acids Res.* 31, 5469–5482.

(13) Michlewski, G., and Krzyzosiak, W. J. (2004) Molecular architecture of CAG repeats in human disease related transcripts. *J. Mol. Biol.* 340, 665–679.

(14) Broda, M., Kierzek, E., Gdaniec, Z., Kulinski, T., and Kierzek, R. (2005) Thermodynamic stability of RNA structures formed by CNG trinucleotide repeats. Implication for prediction of RNA structure. *Biochemistry* 44, 10873–10882.

(15) Yuan, Y., Compton, S. A., Sobczak, K., Stenberg, M. G., Thornton, C. A., Griffith, J. D., and Swanson, M. S. (2007) Muscleblind-like 1 interacts with RNA hairpins in splicing target and pathogenic RNAs. *Nucleic Acids Res.* 35, 5474–5486.

(16) Kiliszek, A., Kierzek, R., Krzyzosiak, W. J., and Rypniewski, W. (2010) Atomic resolution structure of CAG RNA repeats: Structural insights and implications for the trinucleotide repeat expansion diseases. *Nucleic Acids Res.* 38, 8370–8376.

(17) de Mezer, M., Wojciechowska, M., Napierala, M., Sobczak, K., and Krzyzosiak, W. J. (2011) Mutant CAG repeats of Huntingtin transcript fold into hairpins, form nuclear foci and are targets for RNA interference. *Nucleic Acids Res.* 39, 3852–3863.

(18) Vester, B., and Wengel, J. (2004) LNA (locked nucleic acid): High-affinity targeting of complementary RNA and DNA. *Biochemistry* 43, 13233–13241.

(19) Wyatt, J. R., Chastain, M., and Puglisi, J. D. (1991) Synthesis and purification of large amounts of RNA oligonucleotides. *Biotechniques* 11, 764–769.

(20) Mortimer, S. A., and Weeks, K. M. (2007) A fast-acting reagent for accurate analysis of RNA secondary and tertiary structure by SHAPE chemistry. *J. Am. Chem. Soc.* 129, 4144–4145.

(21) Karabiber, F., McGinnis, J. L., Favorov, O. V., and Weeks, K. M. (2012) QuShape: Rapid, accurate, and best-practices quantification of nucleic acid probing information, resolved by capillary electrophoresis. *RNA* 19, 63–73.

(22) Wilkinson, K. A., Merino, E. J., and Weeks, K. M. (2006) Selective 2'-hydroxyl acylation analyzed by primer extension

(SHAPE): Quantitative RNA structure analysis at single nucleotide resolution. *Nat. Protoc.* 1, 1610–1616.

(23) Reuter, J. S., and Mathews, D. H. (2010) RNAstructure: Software for RNA secondary structure prediction and analysis. *BMC Bioinf.* 11, 116.

(24) Deigan, K. E., Li, T. W., Mathews, D. H., and Weeks, K. M. (2009) Accurate SHAPE-directed RNA structure determination. *Proc. Natl. Acad. Sci. U.S.A.* 106, 97–102.

(25) Hajdin, C. E., Bellaousov, S., Huggins, W., Leonard, C. W., Mathews, D. H., and Weeks, K. M. (2013) Accurate SHAPE-directed RNA secondary structure modeling, including pseudoknots. *Proc. Natl. Acad. Sci. U.S.A.* 110, 5498–5503.

(26) Merino, E. J., Wilkinson, K. A., Coughlan, J. L., and Weeks, K. M. (2005) RNA structure analysis at single nucleotide resolution by selective 2'-hydroxyl acylation and primer extension (SHAPE). *J. Am. Chem. Soc.* 127, 4223–4231.

(27) Weeks, K. M., and Mauer, D. M. (2011) Exploring RNA structural codes with SHAPE chemistry. *Acc. Chem. Res.* 44, 1280–1291.

(28) Lin, B., Nasir, J., Kalchman, M. A., McDonald, H., Zeisler, J., Goldberg, Y. P., and Hayden, M. R. (1995) Structural analysis of the 5' region of mouse and human huntington disease genes reveals conservation of putative promoter region and di- and trinucleotide polymorphisms. *Genomics* 25, 707–715.

(29) Lee, J., Park, E. H., Couture, G., Harvey, I., Garneau, P., and Pelletier, J. (2002) An upstream open reading frame impedes translation of the huntingtin gene. *Nucleic Acids Res.* 30, 5110–5119.

(30) Nalavade, R., Griesche, N., Ryan, D. P., Hildebrand, S., and Krau, S. (2013) Mechanisms of RNA-induced toxicity in CAG repeat disorders. *Cell Death Dis.* 4, e752-1–e752-11.

(31) Galka-Marciniak, P., Urbanek, M. O., and Krzyzosiak, W. J. (2012) Triplet repeats in transcripts: Structural insights into RNA toxicity. *Biol. Chem.* 393, 1299–1315.

(32) Hodgson, J. G., Smith, D. J., McCutcheon, K., Koide, H. B., Nishiyama, K., Dinulos, M. B., Stevens, M. E., Bissada, N., Nasir, J., Kanazawa, I., et al. (1996) Human huntingtin derived from YAC transgenes compensates for loss of murine huntingtin by rescue of the embryonic lethal phenotype. *Hum. Mol. Genet.* 5, 1875–1885.

(33) Ehrnhoefer, D. E., Butland, S. L., Pouladi, M. A., and Hayden, M. R. (2009) Mouse models of Huntington disease: Variations on a theme. *Dis. Models & Mech.* 2, 123–129.

(34) Southwell, A. L., Warby, S. C., Carroll, J. B., Doty, C. N., Skotte, N. H., Zhang, W., Villanueva, E. B., Kovalik, V., Xie, Y., Pouladi, M. A., et al. (2013) A fully humanized transgenic mouse model of Huntington disease. *Hum. Mol. Genet.* 22, 18–34.

(35) Slow, E. J., van Raamsdonk, J., Rogers, D., Coleman, S. H., Graham, R. K., Deng, Y., Oh, R., Bissada, N., Hossain, S. M., Yang, Y. Z., et al. (2003) Selective striatal neuronal loss in a YAC128 mouse model of Huntington disease. *Hum. Mol. Genet.* 12, 1555–1567.

(36) Gray, M., Shirasaki, D. I., Cepeda, C., Andre, V. M., Wilburn, B., Lu, X. H., Tao, J., Yamazaki, I., Li, S. H., Sun, Y. E., et al. (2008) Full-length human mutant huntingtin with a stable polyglutamine repeat can elicit progressive and selective neuropathogenesis in BACHD mice. *J. Neurosci.* 28, 6182–6195.

(37) Pouladi, M. A., Stanek, L. M., Xie, Y., Franciosi, S., Southwell, A. L., Deng, Y., Butland, S., Zhang, W., Cheng, S. H., Shihabuddin, L. S., et al. (2012) Marked differences in neurochemistry and aggregates despite similar behavioral and neuropathological features of Huntington disease in full-length BACHD and YAC128 mice. *Hum. Mol. Genet.* 21, 2219–2232.

(38) Sobczak, K., and Krzyzosiak, W. J. (2005) CAG repeats containing CAA interruptions form branched hairpin structures in spinocerebellar ataxia type 2 transcripts. *J. Biol. Chem.* 280, 3898–3910.

(39) Mykowska, A., Sobczak, K., Wojciechowska, M., Kozłowski, P., and Krzyzosiak, W. J. (2011) CAG repeats mimic CUG repeats in the misregulation of alternative splicing. *Nucleic Acids Res.* 39, 8938–8951.

(40) Sathasivam, et al. (2013) Aberrant splicing of HTT generates the pathogenic exon 1 protein in Huntington disease. *Proc. Natl. Acad. Sci. U.S.A.* 110, 2366–2370.

(41) Pickering, B. M., and Willis, A. E. (2005) The implications of structured 5' untranslated regions on translation and disease. *Semin. Cell Dev. Biol.* 16, 39–47.